Journal of Physics: Conference Series **2866** (2024) 012088 doi:10.1088/1742-6596/2866/1/012088

Interference effects in nonequilibrium quantum transport with long-range interactions

Marisa Ulfa[1] and Donny Dwiputra[2]

[1]Department of Physics, Universitas Negeri Jakarta, Jakarta 13220, Indonesia
[2]Research Center for Quantum Physics, National Research and Innovation Agency (BRIN), South Tangerang 15314, Indonesia

E-mail: [1]marisaulfax@gmail.com

Abstract. We investigate how long-range power-law hopping interaction, $\sim 1/r^a$, affects the characteristics of dissipative quantum transport in a nonequilibrium setting. The model under consideration is a noninteracting bosonic chain subject to thermal baths of differing temperature at its boundaries and dephasing noise which is applied uniformly to all the sites. It is shown that the steady-state current may vary nonmonotonically and has a peak for a finite a depending on the position of the cold bath. This site-specific behaviour stems back to the interference effect caused by the parity of the total sites N and the baths positions. The fractional nature of the system, along with the interplay between coherent and incoherent transport, will affect the steady state current that characterizes the transport.

1. Introduction

When a physical system, either classical or quantum, is placed in direct contact with two reservoirs of different temperatures at its edges, it will typically tend to a nonequilibrium steady-state (NESS). In this setting, energy (and particle) is constantly pumped at the hot reservoir to be absorbed at the cold reservoir with finite current. This physical scenario relates to a vast range of major problems in open quantum systems and condensed-matter physics, both theoretically and experimentally, ranging from electron transport in semiconductors [1-3] and mesoscopic systems [4,5], current rectifiers [6,7], dephasing and driven-assisted quantum transport [8-16], to thermal conductivity in gauge/gravity models (AdS/CFT correspondence) [17-19], and even Horndeski's gravity [20]. NESS also plays crucial role in biological building blocks such as DNA and protein, whose complex dynamics can be studied classically [21-25] or in quantum regime [26-28], particularly in open systems setting [29-37].

Low-dimensional lattice of spins and fermions have become a powerful experimental playground in recent years, mainly due to the rapid advances in experiments with 1D and 2D quantum simulators, e.g., ultracold atoms [38,39], trapped ions [15], and photonic networks [14]. Traditionally, the intersite (or hopping) interaction in these systems is modeled with nearest-neighbour coupling. However, coupling in any realistic systems is in long ranged, in which power-law interaction, $1/r^a$, is one of the most common form. Dipole-dipole interactions ($\sim 1/r^3$) play a central role for polar molecules [40], magnetic atoms [41], and nitrogen-vacancy centers [42]. Furthermore, tunable fractional power-law effective interactions ($0 \leq a \leq 3$) are available in several systems [43,44], each having interesting non-local entanglement and quantum correlation transfer properties. In disordered potentials, self-duality breaking quasicrystals with power-law hopping possess rich localization properties and a hiearchy of multifractality which heavily dependent on the exponent a [45]. Yet, the study of nonequilibrium open system transport with power-law interaction has apparently been understudied.

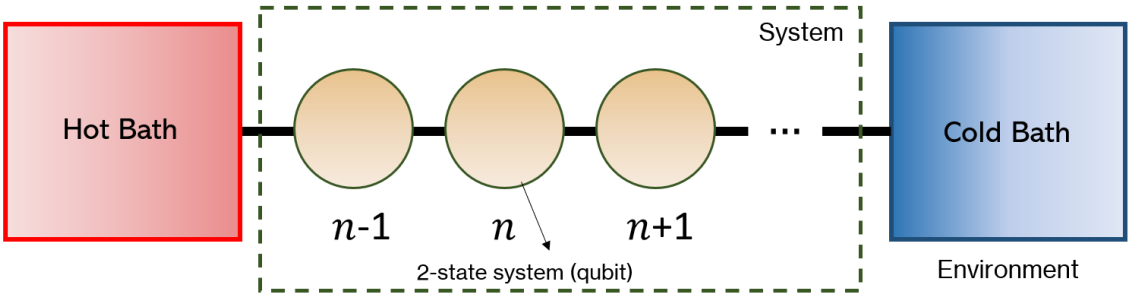

Figure 1. Schematics of the open quantum system considered in this paper. N linear two level systems with long-range hopping is coupled to hot and cold baths at its ends.

In this paper, we study the nonequilibrium transport of a clean (disorder-free) 1D lattice which facilitates the transfer of a noninteracting particle with power-law hopping. Our model is the simplest as possible so that we can isolate the sole effect of the power-law interaction to the transport. We found that the particle current varies nonmonotonically with respect to the power-law exponent a, meaning that there exists an optimum exponent which enhances transport the most. This enhancement behaviour strongly depends on the choice of which site is coupled to the cold reservoir, which we refer to as the exit site of the particle.

2. Model

We consider a clean 1D lattice of $\boldsymbol{N}$ coupled bosonic modes in a tight-binding model using second-quantisation language, which is commonly used in modern literatures,

$$H(t) = -\sum_{n<m}^{N} J_{n-m}(a_n^+ a_m + H.c.), \tag{1}$$

where $a_n^+(a_n)$ is the usual bosonic creation (annihilation) operator at site n. The hopping (or tunneling) rate J_{n-m} takes the power-law form which decays over the distance $n-m$,

$$J_{n-m} = \frac{J}{|n-m|^a}. \tag{2}$$

In this paper we set $\hbar = 1$ and take J as the unit of energy.

The system is coupled to two different environments: pair of thermal reservoirs (baths) of noninteracting bosons at different temperature; see figure 1. The hot bath is coupled to the $n = 1$ site, while the cold bath is to the 1-th site. We will vary the latter site to see the response in the transport properties. The environmental coupling is modeled by a phenomenological-local [46,47] Markovian master equation [48],

$$\dot{\rho}(t) = -i[H,\rho] + \mu_{in}\mathcal{D}_{in}[a_1^+]\rho + \rho_{out}\mathcal{D}_{out}[a_l]\rho, \tag{3}$$

where $\rho(t)$ is the density matrix, and $\mathcal{D}[L]\cdot = L\cdot L^+ - \frac{1}{2}\{L^+L, \cdot\}$ is the Gorini-Kossakowski-Sudarshan-Lindblad (GKSL) dissipator of the Lindbladian L [49,50]. Here, μ_{in} and μ_{out} are the particle injection and exit rates, respectively.

To quantify the transport, we calculate the particle current [51],

$$\mathcal{J} = -Tr(\mathcal{N}D_{out}\rho_{NESS}), \tag{4}$$

where $\mathcal{N} = \sum_n a_n^+ a_n$ is the total particle number operator, $\mathcal{D}_{\text{out}}\rho$ is the dissipators acting on the exit site l, and ρ_{NESS} is the NESS density matrix, obtained by solving $\dot{\rho} = 0$ [see equation (3)]. One can

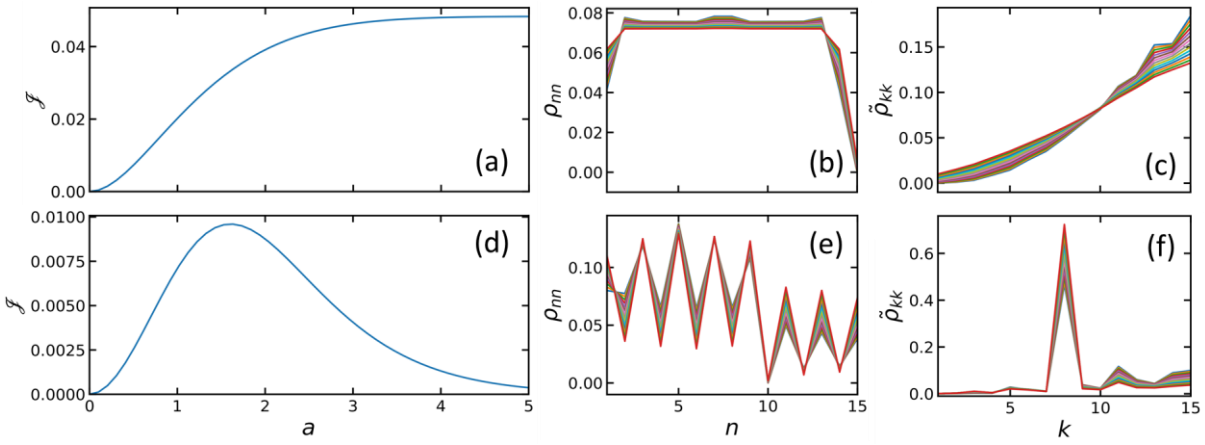

Figure 2. Transport properties for $N = 15$ and $\mu = 5J$. For row (a)—(c), exit site $l = N$; for row (d)—(f), $l = 10$. Column (a),(d): particle current $\mathcal{J}$ (in units of J) v.s. exponent a. Column (b),(e): Site-basis population ρ_{nn}. Column (c),(f): Eigenbasis population. The population graphs are superimposed from $a = 0^+$ to $a = 5$ (with color variations).

simply show, using the commutation relation $[a_i, a_j^+] = \delta_{ij}$ and the operator in 1-particle manifold $a_n = |0\rangle\langle n|$, that the particle current is proportional to the exit site population of the NESS,

$$\mathcal{J} = \mu_{out}\langle l|\rho_{NESS}|l\rangle. \tag{5}$$

Note that for the closed system the particle number is conserved, since $[H, \mathcal{N}] = 0$. Thus the change of particle number in the chain is only done by the Lindblad dissipators, by the annihilation and creation operators. However, there are several cases that a 1-particle manifold consideration is valid. The common wisdom is when the injection rate is low, $\mu_{\text{in}}/\mu_{\text{out}} \ll 1$, or alternatively when $\mu_{\text{in}}/\mu_{\text{out}} = 1$ but with average particle number [43],

$$\langle \mathcal{N} \rangle = \frac{K}{K+1}, \quad K = N + \frac{N+1}{4}\frac{\mu_{out}^2}{J}, \tag{6}$$

close to 1. For this paper we tune the parameter μ_{out} so that the latter case is satisfied. This way, one can safely use the 1-particle manifold. Note that this expression for $\langle \mathcal{N} \rangle$ is originally derived for a clean nearest-neighbour nonequilibrium model. Nevertheless, nearest-neighbour hopping is the large exponent limit $a \to \infty$ of the power-law model, so that the particle number for hoppings softer than this case should behave similarly.

3. Results and discussions

The NESS is obtained numerically by solving $\dot{\rho} = 0$ using `QuTiP` package in Python 3.x. For brevity, from hereafter we simply refer to ρ_{NESS} as ρ. We take the common injection/exit rates, $\mu_{\text{in}} = \mu_{\text{out}} = \mu$. Figure 1(a) and (c) shows the particle current $\mathcal{J}$ for chains with exit site $l = N = 15$ (end site) and $l = 10$, respectively. For the one with end-to-end transport ($l = N$) the current profile is asymptotically increasing along a. The highest value is obtained for large a, or equivalently, for the limit of nearest-neighbour hopping. This behaviour is typical for larger chains, albeit with smaller current; the scaling exponent of which (with respect to N) should be clarified further by analytically calculating the current for nearest-neighbour case, which is actually a reasonable calculation.

If the exit site is not the last site, figure 2(d), interestingly the current increases nonmonotonically, i.e., there is an optimum value of a, while for the nearest-neighbour limit the current vanishes. To understand why this happens, we plot the NESS population ρ_nn in figure 2(b) and (e). For the end-to-end transport, apart from the uniform plateau, population gradients are apparent, particularly near the end site, while for $l = 10$ the interference pattern is prominent even in the steady-state. The apparence

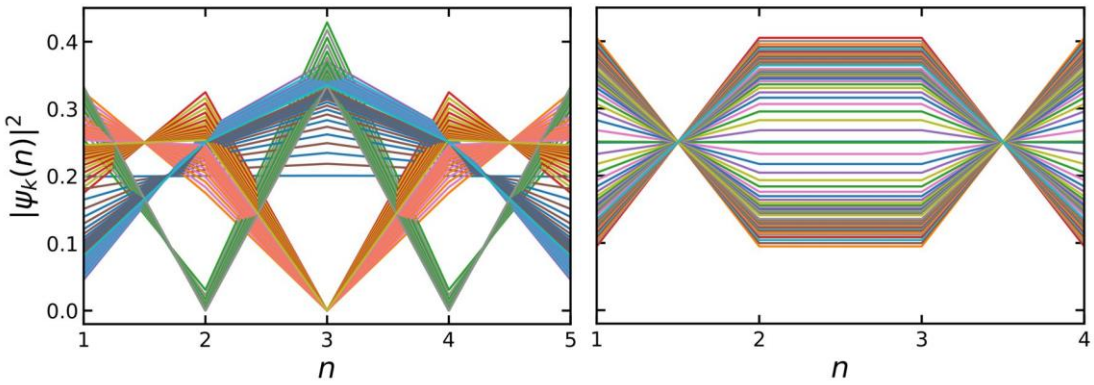

Figure 3. Eigenstates occupation, $|\psi_k(n)|^2$, of short chains (for ease of viewing) with (left) $N = 5$ and (right) $N = 4$. The graphs are superimposed with varying the long-range exponent $a = 0^+$ to $a = 5$ (color variations). Notice that for odd total sites N, the center site occupation is always an extreme node (zero or maxima), whike for even N this node does not exist.

of population gradient should not be confused as the emergence of Fick's law diffusion (formation of population gradient) since we are not incorporating dephasing noise, which triggers the quantum-to-classical transition.

Why $l = 10$ is special; is there other l that gives the current peak? To answer this, we shall observe the NESS population in eigenbasis, denoted by $\tilde{\rho}_{kk}$ with the eigenstates $|\psi_k\rangle = \sum_n \psi_k(n)|n\rangle$. For end-to-end transport $\tilde{\rho}_{kk}$, figure 2(c) shows a relatively monotonic profile with the maximum occupation is at the highest eigenstate. This is in contrast with figure 2(f), for $l = 10$, where there is a dominant eigenstate governing the steady-state. Since particle current is proportional to the exit site population, the dominant eigenstate must have a node of zero (or almost zero) occupation in the exit site. When a increases, this occupation shifts upwards. Even a minute shift can result in huge variation of the current (compared to zero; for monotonic behaviour at $a \to 0$ and $a \to \infty$).

The next logical step is to show whether the prominent eigenstate in figure 2(f) has a node for the exit site occupation, i.e. whether $|\psi_k(l)|^2 = 0$ for the k-th eigenstates corresponding to the prominent one—indeed it is (not shown here). In fact, the deduction is actually the reverse: *if the eigenstates of H have node at the exit site, the current will have peak with respect to the exponent* a. However, plotting all the eigenstates for $N = 15$ is unpleasing for the eye. Thus we plot all the eigenstates of the closed system, without the dissipators, for shorter chains, $N = 4$ and $N = 5$ in figure 3. For instance, we see there is a node in figure 3(left) at $n = 4$. If we take this as the exit site l, we shall get the current profile like in figure 2(b). Interestingly, for odd total number of sites N only, if l is set as the center site then $\mathcal{J}$ is always zero for all a. This is due to the parity symmetry of the system; chains with even N do not have this property. The eigenstates at the center site always have zero and a maximum node, also for larger chains with odd N. Now, what happen if the eigenstates do not contain node at all, such as in figure 3(right)? In this case the only possible behaviour for $\mathcal{J}$ is monotonic, such as in figure 2(a).

Finally, we note that for larger N, the current profile may contain more peak. Further study needs to check first, whether the number of peaks is at all correlated with the number of prominent eigenstates occupation of the steady-state. So far we have analysed the connection between the nodes in the eigenstates occupation and the nonmonotonicity of the current. This connection is in a sense similar to the disorder-assisted quantum transport, where finite (nonzero) disorder may, counterintuitively, increase the current [52]. Also for the exit site that coincides with the eigenstate nodes, current peak appears. The remaining question is that why the current converge to either a finite value or to zero in the first place, and also, why the eigenstates respond to variation in a in such way that the population ρ_{ll} behaves nonmonotonically. These can be answered for $a \to \infty$ by analytical calculations, which surely gives progress toward general a.

4. Conclusion

Finally, we note that for larger $\boldsymbol{N}$, the current profile may contain more peak. Further study needs to check first, whether the number of peaks is at all correlated with the number of prominent eigenstates occupation of the steady-state. So far we have analysed the connection between the nodes in the eigenstates occupation and the nonmonotonicity of the current. This connection is in a sense similar to the disorder-assisted quantum transport, where finite (nonzero) disorder may, counterintuitively, increase the current [52]. Also for the exit site that coincides with the eigenstate nodes, current peak appears. The remaining question is that why the current converge to either a finite value or to zero in the first place, and also, why the eigenstates respond to variation in $\boldsymbol{\alpha}$ in such way that the population $\boldsymbol{\rho_{ll}}$ behaves nonmonotonically. These can be answered for $\boldsymbol{\alpha \to \infty}$ by analytical calculations, which surely gives progress toward general $\boldsymbol{\alpha}$.

References

[1] Jacoboni C 2010 *Theory of electron transport in semiconductors: a pathway from elementary physics to nonequilibrium Green functions* vol 165 (Springer Science & Business Media)
[2] Coropceanu V, Cornil J, da Silva Filho D A, Olivier Y, Silbey R and Brédas J L 2007 Charge transport in organic semiconductors *Chem. Rev.* **107** 926–952
[3] Nag B R 2012 *Electron transport in compound semiconductors* vol 11 (Springer Science & Business Media)
[4] Baringhaus J, Ruan M, Edler F, Tejeda A, Sicot M, Taleb-Ibrahimi A, Li A P, Jiang Z, Conrad E H, Berger C et al. 2014 Exceptional ballistic transport in epitaxial graphene nanoribbons *Nature* **506** 349–354
[5] Dwiputra D and Zen F P 2022 Single-particle mobility edge without disorder *Phys. Rev.* B **105** L081110
[6] Balachandran V, Clark S R, Goold J and Poletti D 2019 Energy current rectification and mobility edges *Phys. Rev. Lett.* **123** 020603
[7] Saha M and Maiti S K 2019 Particle current rectification in a quasi-periodic double-stranded ladder *J. Phys.* D *Appl. Phys.* **52** 465304
[8] Dwiputra D, Sulaiman A, Kosasih J S, Hidayat W and Zen F P 2019 Driving the dephasing assisted quantum transport *J. Phys.: Conf. Ser.* **1245** 012075
[9] Dwiputra D, Kosasih J S, Sulaiman A and Zen F P 2020 Driving-assisted open quantum transport in qubit networks *Phys. Rev.* A **101** 012113
[10] Dwiputra D and Zen F P 2021 Environment-assisted quantum transport and mobility edges *Phys. Rev*. A **104** 022205
[11] Mohseni M, Rebentrost P, Lloyd S and Aspuru-Guzik A 2008 Environment-assisted quantum walks in energy transfer of photosynthetic complexes *J. Chem. Phys.* **129** 11B603
[12] Sowa J K, Mol J A, Briggs G A D and Gauger E M 2017 Environment-assisted quantum transport through single-molecule junctions *Phys. Chem. Chem. Phys.* **19** 29534–29539
[13] Schempp H, Günter G, Wüster S, Weidemüller M and Whitlock S 2015 Correlated exciton transport in Rydberg-dressed-atom spin chains *Phys. Rev. Lett.* **115** 093002
[14] Biggerstaff D N, Heilmann R, Zecevik A A, Gräfe M, Broome M A, Fedrizzi A, Nolte S, Szameit A, White A G and Kassal I 2016 Enhancing coherent transport in a photonic network using controllable decoherence *Nat. Comm.* **7** 11282
[15] Trautmann N and Hauke P 2018 Trapped-ion quantum simulation of excitation transport: Disordered, noisy, and long-range connected quantum networks *Phys. Rev.* A **97** 023606
[16] Maier C, Brydges T, Jurcevic P, Trautmann N, Hempel C, Lanyon B P, Hauke P, Blatt R and Roos C F 2019 Environment-assisted quantum transport in a 10-qubit network *Phys. Rev. Lett.* **122** 050501
[17] Hartnoll S A, Lucas A and Sachdev S 2018 *Holographic quantum matter* (MIT press)
[18] Prihadi H L, Zen F P, Dwiputra D and Ariwahjoedi S 2023 Chaos and fast scrambling delays of a dyonic Kerr-Sen-AdS$_4$ black hole and its ultraspinning version *Phys. Rev.* D **107** 124053

[19] Prihadi H L, Zen F P, Dwiputra D and Ariwahjoedi S 2024 Localized chaos due to rotating shock waves in Kerr–AdS black holes and their ultraspinning version *Gen. Relativ. Gravit.* **56** 90
[20] Baggioli M and Li W J 2017 Diffusivities bounds and chaos in holographic Horndeski theories *J. High Energy Phys.* **2017** 1–26
[21] Dwiputra D, Hidayat W, Khairani R and Zen F 2016 Nonlinear dynamics of specific DNA-protein interactions *J. Phys.: Conf. Ser.* **694** 012076
[22] Dwiputra D, Hidayat W, Khairani R and Zen F 2016 Nonlinear Model of the Specificity of DNA-Protein Interactions and Its Stability *J. Phys.: Conf. Ser.* **739** 012030
[23] Dwiputra D, Hidayat W and Zen F P 2017 Nonlinear dynamics of DNA bubble induced by site specific DNA-protein interaction *J. Phys.: Conf. Ser.* **856** 012005
[24] Khairani R, Dwiputra D, Hidayat W and Zen F P 2019 Effect of Solvent on Stretching and Twisting of DNA *J. Phys.: Conf. Ser.* **1127** 012013
[25] Dwiputra D, Hidayat W and Zen F P 2019 Low Amplitude Kink Soliton Excitation in Peyrard-Bishop Double Strand DNA Model *J. Phys.: Conf. Ser.* **1204** 012008
[26] Lambert N, Chen Y N, Cheng Y C, Li C M, Chen G Y and Nori F 2013 Quantum biology *Nat. Phys.* **9** 10–18
[27] Cao J, Cogdell R J, Coker D F, Duan H G, Hauer J, Kleinekathöfer U, Jansen T L, Mančal T, Miller R D, Ogilvie J P et al. 2020 Quantum biology revisited *Sci. Adv.* **6** eaaz4888
[28] Stuchebrukhov A A 2003 Long-distance electron tunneling in proteins *Theor. Chem. Acc.* **110** 291–306
[29] Mori T and Shirai T 2023 Symmetrized Liouvillian gap in Markovian open quantum systems *Phys. Rev. Lett.* **130** 230404
[30] Xue P, Lin Q, Wang K, Xiao L, Longhi S and Yi W 2024 Self acceleration from spectral geometry in dissipative quantum-walk dynamics *Nat. Commun.* **15** 4381
[31] Van V T, Vo V T and Saito K 2024 Dissipation, quantum coherence, and asymmetry of finite-time cross-correlations *Phys. Rev. Res.* **6** 013273
[32] Mori T 2024 Liouvillian-gap analysis of open quantum many-body systems in the weak dissipation limit *Phys. Rev.* B **109** 064311
[33] Nathan F and Rudner M S 2020 Universal Lindblad equation for open quantum systems *Phys. Rev.* B **102** 115109
[34] Tupkary D, Dhar A, Kulkarni M and Purkayastha A 2022 Fundamental limitations in Lindblad descriptions of systems weakly coupled to baths *Phys. Rev.* A **105** 032208
[35] Dhawan A, Ganguly K, Kulkarni M and Agarwalla B K 2024 Anomalous transport in long-ranged open quantum systems *Phys. Rev.* B **110** L081403
[36] Nathan F and Rudner M S 2024 Quantifying the accuracy of steady states obtained from the universal Lindblad equation *Phys. Rev.* B **109** 205140
[37] Anto-Sztrikacs N, Nazir A and Segal D 2023 Effective-Hamiltonian theory of open quantum systems at strong coupling *PRX Quantum* **4** 020307
[38] Wall M L 2015 *Quantum many-body physics of ultracold molecules in optical lattices: Models and simulation methods* (Springer)
[39] Liu D E, Levchenko A and Baranger H U 2013 Floquet Majorana Fermions for Topological Qubits in Superconducting Devices and Cold-Atom Systems *Phys. Rev. Lett.* **111** 047002
[40] Yan B, Moses S A, Gadway B, Covey J P, Hazzard K R, Rey A M, Jin D S and Ye J 2013 Observation of dipolar spin-exchange interactions with lattice-confined polar molecules *Nature* **501** 521–525
[41] De Paz A, Sharma A, Chotia A, Marechal E, Huckans J, Pedri P, Santos L, Gorceix O, Vernac L and Laburthe-Tolra B 2013 Nonequilibrium quantum magnetism in a dipolar lattice gas *Phys. Rev. Lett.* **111** 185305
[42] Waldherr G, Wang Y, Zaiser S, Jamali M, Schulte-Herbrüggen T, Abe H, Ohshima T, Isoya J, Du J, Neumann P et al. 2014 Quantum error correction in a solid-state hybrid spin register *Nature* **506** 204–207

[43] Richerme P, Gong Z X, Lee A, Senko C, Smith J, Foss-Feig M, Michalakis S, Gorshkov A V and Monroe C 2014 Non-local propagation of correlations in quantum systems with long-range interactions *Nature* **511** 198–201
[44] Jurcevic P, Lanyon B P, Hauke P, Hempel C, Zoller P, Blatt R and Roos C F 2014 Quasiparticle engineering and entanglement propagation in a quantum many-body system *Nature* **511** 202–205
[45] Deng X, Ray S, Sinha S, Shlyapnikov G and Santos L 2019 One-dimensional quasicrystals with power-law hopping *Phys. Rev. Lett.* **123** 025301
[46] González J O, Correa L A, Nocerino G, Palao J P, Alonso D and Adesso G 2017 Testing the validity of the 'local' and 'global' GKLS master equations on an exactly solvable model *Open Syst. Inf. Dyn.* **24** 1740010
[47] Hofer P P, Perarnau-Llobet M, Miranda L D M, Haack G, Silva R, Brask J B and Brunner N 2017 Markovian master equations for quantum thermal machines: local versus global approach *New J. Phys.* **19** 123037
[48] Breuer H P and Petruccione F 2002 *The theory of open quantum systems* (Oxford University Press)
[49] Gorini V, Kossakowski A and Sudarshan E C G 1976 Completely positive dynamical semigroups of N-level systems *J. Math. Phys.* **17** 821–825
[50] Lindblad G 1976 On the generators of quantum dynamical semigroups *Comm. Math. Phys.* **48** 119–130
[51] Wu L A and Segal D 2008 Energy flux operator, current conservation and the formal Fourier's law *J. Phys. A Math. Theor.* **42** 025302
[52] Zerah-Harush E and Dubi Y 2020 Effects of disorder and interactions in environment assisted quantum transport *Phys. Rev. Res.* **2** 023294